Journal of Magnetism and Magnetic Materials 489 (2019) 165406

Contents lists available at ScienceDirect

Journal of Magnetism and Magnetic Materials

journal homepage: www.elsevier.com/locate/jmmm

Research articles

Influence of the dipolar interaction in the creation of skyrmions in coupled nanodisks

H. Vigo-Cotrina, A.P. Guimarães

Centro Brasileiro de Pesquisas Físicas, 22290-180 Rio de Janeiro, RJ, Brazil

ARTICLE INFO

Keywords:
Néel skyrmion
Pulse polarized current
Coupled nanodisks
Micromagnetic simulation

ABSTRACT

In the present work, using micromagnetic simulation, we show that the dipolar magnetic interaction effect plays a very important role in the process of creation of skyrmions in a coupled system of nanodisks. First, we have determined the magnetic ground state in an isolated nanodisk for different values of perpendicular uniaxial anisotropy (PUA) and Dzyaloshinskii-Moriya interaction (DMI). Next, we have applied perpendicular pulse polarized current densities (J) and found that it is possible to create a metastable Néel skyrmion from a nanodisk whose ground state is a single magnetic domain. From these results, we obtained a phase diagram of polarized current intensity vs. time of application of the current pulses, for different values of parameters such as PUA, DMI, and distance between the nanodisks. Our results show that, depending on the separation distance between the nanodisks, the current density required to create a skyrmion changes, due to the dipolar magnetic interaction.

1. Introduction

Magnetic skyrmions are non-trivial spin textures that can appear in ferromagnets (FM) where there is lacking inversion symmetry [1–4]. In ultrathin film multilayer systems (FM/substrate), the Dzyaloshinskii-Moriya interaction (DMI) is the main responsible for the creation of skyrmions [1,2,5]. This DMI has its origin in the interface of the multilayer due to strong spin-orbit coupling between FM and the substrate [1,4].

There are two skyrmion types: Bloch skyrmion and Néel skyrmion [1,2,4]. The first is generally encountered in bulk systems, while the latter is present in multilayer systems [3,4]. Mathematically, a skyrmion is quantified by the topological Charge Q, which is defined by $Q = (1/4\pi)\int \mathbf{m}.(\partial_x \mathbf{m} \times \partial_y \mathbf{m})\, dxdy$, where $\mathbf{m}$ is the reduced magnetization. $Q = \pm 1$ for skyrmions [1,6].

Several works have shown that a skyrmion can be stabilized in geometries as, for example, disks [3,7,8], ultrathin films [9], and racetracks [10,11]. However, it is also possible to create a multiskyrmion cluster in a single nanodisk [12,13]. Skyrmions can also be created with the help of external perturbations, such as magnetic field [14–16], spin polarized current [3,17,18], or local heating [19].

Due to the fact that skyrmions are topologically protected stable magnetic structures [20,2,3], and can be moved with small current densities, of the order of 10^6 A/m^2[21], they have many potential applications, e.g., as logic gate devices [10], racetrack memories [11,22], or spin-torque nano-oscillators (STNOs) [23,24].

Nanodisks with magnetic skyrmions have been object of many studies [12,23,25], since these systems can be used to produce microwave [26], or spin wave based computing and logic devices [25].

For technological applications, the nanostructures are normally organized in arrays. This leads to the question of magnetic interaction between them. There are in the literature several works about the creation and stabilization of skyrmions in isolated structures [3,7,8,18,23,24,27], but work is still lacking on the role of magnetic interaction in the process of creation of a skyrmion. The aim of this work is to study the effect of the magnetic dipolar coupling in the creation of a Néel skyrmion in a thin nanodisk system. For this purpose, we tailored the perpendicular uniaxial anisotropy (PUA), Dzyaloshinskii-Moriya interaction (DMI) and polarized current density (J) in the ultrathin nanodisk (isolated and coupled systems). We used the open source software Mumax3 [28], with cell size of $1 \times 1 \times L$ nm^3, where L is the thickness of the nanodisk. The material used is Cobalt with parameters [3,9,18]: saturation magnetization $M_s = 5.8 \times 10^5$ A/m, exchange stiffness $A = 1.5 \times 10^{-11}$ J/m, and damping constant $\alpha = 0.3$ (for faster convergence). The perpendicular uniaxial anisotropy constant (K_z) and Dzyaloshinskii-Moriya exchange constant (D_{int}) varied from 0.4 to 1.8 MJ/m^3 and from 3 to 4.5 mJ/m^2, respectively [3,7,27].

2. Results and discussion

2.1. Isolated nanodisk

We considered a nanodisk (see Fig. 1) with thickness L = 0.4 nm and diameter D = 80 nm. The pulse current density is polarized in the direction $\mathbf{m}_p = (1, 0, 0)$.

https://doi.org/10.1016/j.jmmm.2019.165406
Received 14 April 2019; Received in revised form 21 May 2019; Accepted 3 June 2019
Available online 04 June 2019

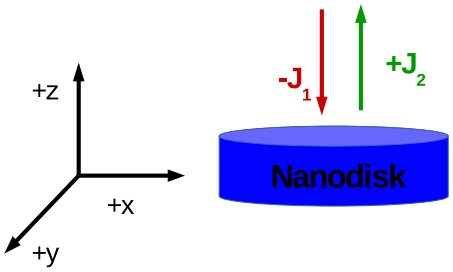

Fig. 1. Schematic representation of a nanodisk. J_1 and J_2 are the densities of the spin currents flowing through the nanodisk.

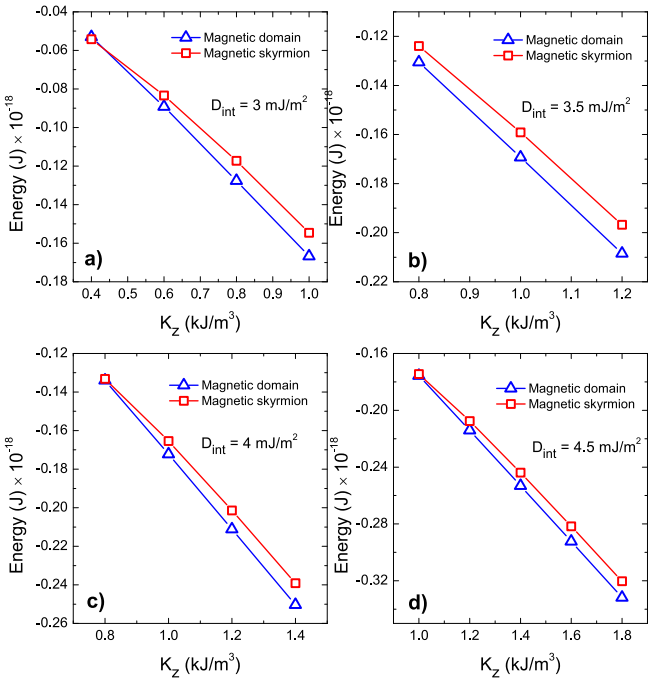

Fig. 2. Energy of the magnetic final states of the nanodisk vs. perpendicular uniaxial anisotropy constant (K_z).

First, in order to determine the magnetic ground state of the nanodisk ($J = 0\,A/m^2$), we considered in our micromagnetic simulations two initial magnetic configurations: perpendicular magnetic domain and Néel skyrmion. The energies of the final magnetic states are shown in Fig. 2 for values of DMI, from $D_{int} = 3\,mJ/m^2$ to $D_{int} = 4.5\,mJ/m^2$. We have considered only cases where both perpendicular magnetic domain (PMD) and magnetic Néel skyrmion (MNS) can be obtained as final magnetic states. For example, for $D_{int} = 3\,mJ/m^2$ (see Fig. 2(a)), the region where it is possible to obtain PMD and MNS as final magnetic states is between $K_z = 0.4\,MJ/m^3$ and $K_z = 1\,MJ/m^3$. For values below $K_z = 0.4\,MJ/m^3$ (not shown here), there is only one single final magnetic state, that is the magnetic skyrmion, and for values greater that $1\,MJ/m^3$ (not shown here), the only final magnetic state is the perpendicular magnetic domain.

The same behavior occurs for all other cases shown in Fig. 2,[1] for $D_{int} = 3.5$, 4 and $4.5\,mJ/m^2$, with their respective ranges of K_z values.

Once established the ranges of values of quantities such as K_z and D_{int}, we proceed to create a metastable Néel skyrmion from the state of lower energy (perpendicular magnetic domain) following the methodology used by Yuan *et al.* [18].

There are two density currents[2] to be used (see Fig. 1): $-J_1$ (current flowing in the $-z$ direction) and $+J_2$ (current flowing in the $+z$ direction). We used $|J_1|$, $|J_2|$ between $0.8\times10^{12}\,A/m^2$ and $3\times10^{12}\,A/m^2$. The first was applied in order to flip the magnetization to the plane of the nanodisk, in the $-x$ direction, and the last to change the direction to $+x$. Depending on the value of J_1 and the time duration and the value of the current density pulse $+J_2$, it is possible to create a metastable Néel skyrmion in the nanodisk.

Unlike the work of Yuan *et al.* [18], where only one case is shown, for $|J_1| = |J_2| = 2\times10^{12}\,A/m^2$, we here show that considering $|J_1| \neq |J_2|$, it is also possible to obtain a MNS. We have also expanded the range of parameters (several values of PUA, DMI, and J), to obtain several phase diagrams (this article and Supplementary material contain 77 phase diagrams) illustrating the conditions of creation of a skyrmion in an isolated, and in coupled nanodisks. The topological charge Q was measured in every case to verify if the structure was a skyrmion.

Following the methodology of Ref. [18], we start with a perpendicular single domain structure (Fig. 3(a) and (f)). A sequence of pulse currents $-J_1$ and $+J_2$ are used to flip the magnetization[3] in the -x direction (Fig. 3(b) and (g)), and the $+x$ direction respectively. Controlling the duration of the application of $+J_2$, it is possible to create a skyrmion (Fig. 3(c, d) and (h, i)). Once the skyrmion is created, the system is allowed to relax[4] with $J_2 = 0$ (Fig. 3(e) and (j)).

The phase diagrams for the cases $K_z = 0.6\,MJ/m^3$, $K_z = 0.8\,MJ/m^3$ and $D_{int} = 3\,mJ/m^2$ are shown in Fig. 4 for different values of J_1. It is possible to observe that the phase diagram is also modified by the value of J_1, since J_1 controls the flipping of the magnetic moments to the plane of the nanodisk. For example, for $K_z = 0.8\,MJ/m^3$ and $J_1 = -1.4\times10^{12}\,A/m^2$ (Fig. 4(c)), we have obtained a metastable Néel skyrmion[5] for almost the entire range of current duration used here. However, when this value was modified to $J_1 = -2.8\times10^{12}\,A/m^2$ (Fig. 4(d)), the phase diagram changes drastically. A similar result is obtained for the case $K_z = 0.6\,MJ/m^3$ (Fig. 4(a, b)).

For all values of K_z and D_{int} used here, we have obtained phase diagrams that are dependent on J_1, J_2 and duration of the current pulse. However, we have not encountered a direct relation between the values J_1, J_2 and K_z, D_{int} in the creation of a metastable skyrmion. The phase diagrams are highly non-linear, nevertheless, it is possible to find some general patterns in the formation of a skyrmion (see Fig. 11 in the Supplementary material[6]). For example, for the cases where $D_{int} = 3.5\,mJ/m^2$, a magnetic skyrmion can be created from a current density threshold[7] of $|J_1| = 1.4\times10^{12}\ A/m^2$ for $K_z = 0.8\times10^{12}\,MJ/m^3$ (Fig. 11 in SP), but when K_z increases to $K_z = 1\,MJ/m^3$, the current density threshold to increase to $|J_1| = 1.8\,A/m^2$ (Fig. 11 in SP). For $K_z = 1.2\,MJ/m^3$, it is not possible anymore to create a skyrmion with the values of density currents used in this work. The same behavior was found for $D_{int} = 4\,mJ/m^2$, the current density threshold increases from $|J_1| = 1.2\times10^{12}\,A/m^2$ (for $K_z = 0.8\,MJ/m^3$) to $|J_1| = 1.6\times10^{12}\,A/m^2$ (for $K_z = 1\,MJ/m^3$) and for $K_z = 1.4\,MJ/m^3$, the current density threshold increases up to $|J_1| = 2.8\times10^{12}\,A/m^2$. This increase in the

[1] The cases for $D_{int} = 2.5\,mJ/m^2$ and $D_{int} = 5\,mJ/m^2$ (not shown here) have presented the same behavior.

[2] The Oersted fields do not influence the creation of skyrmions (in our case), as has already been demonstrated by Yuan *et al.* [18]

[3] The flipping of the magnetization is possible due to the Slonczewski torque, with micromagnetic parameters: $\Lambda = 2$ (Slonczewski asymmetry) and $\epsilon' = 0.2$ [18], exerted by the pulse current on the magnetic moments in the nanodisk.

[4] In most of the works on the creation of skyrmions, it is required that the external perturbation (e.g., magnetic field, current density) is not turned off, since otherwise, the skyrmion vanishes. In our case, the perturbation (perpendicular current density pulses) is turned off and the skyrmion remains stable in the nanodisk.

[5] The skyrmions may have polarity $p = +1$ or $p = -1$.

[6] Supplementary material is abbreviated as SP.

[7] We focus our attention on J_1, since this current density is the one that is responsible for giving the initial condition to our system.

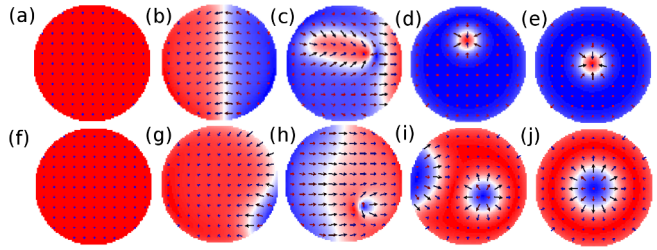

Fig. 3. Evolution of the z-component of the magnetization configuration from the initial perpendicular single domain to the creation of a metastable Néel skyrmion, for $D_{int} = 3\,mJ/m^2$ and (a–e) $K_z = 0.8\,MJ/m^3$ and (f–j) $K_z = 0.6\,MJ/m^3$.

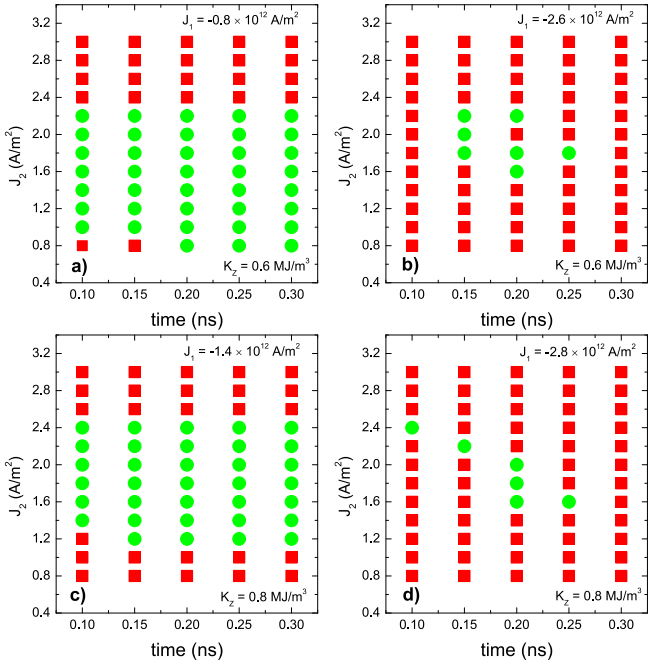

Fig. 4. Phase diagram of J_2 versus its duration, for $K_z = 0.6\,MJ/m^3$, $K_z = 0.8\,MJ/m^3$ and $D_{int} = 3\,mJ/m^2$, and different values of the current density J_1. Red squares indicate no creation of skyrmion, and green circles indicate creation of skyrmion. (For interpretation of the references to colour in this figure legend, the reader is referred to the web version of this article.)

values of current density threshold is due to the fact that higher values of J_1 are necessary in order to flip the magnetization to the plane, in order to overcome the perpendicular alignment due to the presence of K_z.

On the other hand, it is possible to observe how the increase of D_{int} favors the decrease of the current density threshold $|J_1|$. For example, for $K_z = 0.8\,MJ/m^3$ (Fig. 11 in SP), $|J_1|$ decreases from $|J_1| = 1.4 \times 10^{12}\,A/m^2$ ($D_{int} = 3\,mJ/m^2$) to $|J_1| = 1.2 \times 10^{12}\,A/m^2$ ($D_{int} = 4\,mJ/m^2$). The similar behavior is observed for $K_z = 1\,MJ/m^3$, where $|J_1|$ decreases from $|J_1| = 2.6 \times 10^{12}\,A/m^2$ ($D_{int} = 3\,mJ/m^2$) to $|J_1| = 1.4 \times 10^{12}\,A/m^2$ ($D_{int} = 4.5\,mJ/m^2$).

In all cases, the skyrmions have topological charge $Q \approx 1$. Q is not exactly one, because our disks have finite size.

An interesting case occurs for $K_z = 0.8\,MJ/m^3$, $D_{int} = 3\,mJ/m^2$, $J_1 = -3 \times 10^{12}\,A/m^2$, $J_2 = 2.4 \times 10^{12}\,A/m^2$ and duration time of $t = 0.10\,ns$ for J_2 (not shown here): we have obtained two skymions, as final magnetic configuration, in the nanodisk, both with polarity $p = +1$ (in this case the topological charge Q is approximately two).

For some combinations of K_z, D_{int}, J_1 and J_2, we have obtained as final states strange magnetic configurations (similar to that shown in Fig. 3(i)) where a skyrmion coexists with a magnetic domain. These

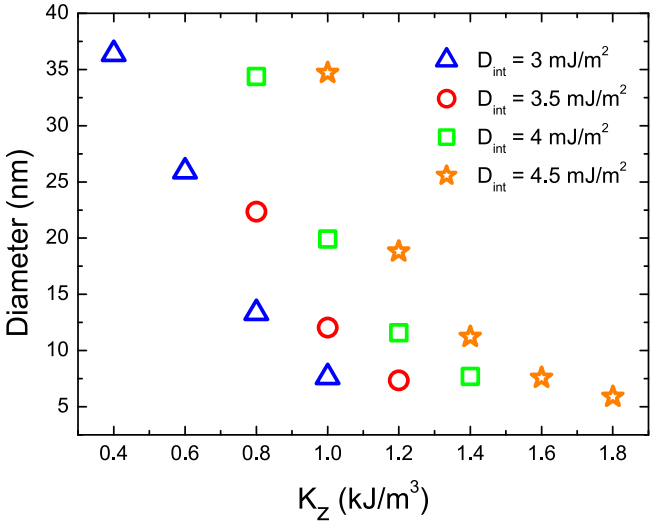

Fig. 5. Skyrmion diameter D_N as a function of the values of the perpendicular anisotropy constant K_z, and Dzyaloshinskii-Moriya exchange constant D_{int}.

cases cannot be considered as pure Néel Skyrmions. Similar configurations have been obtained in cobalt disks under application of perpendicular magnetic fields, as already shown by Talapatra *et al.* [29].

We have obtained the average Néel skyrmion diameters (D_N), considering as the diameter, the dimension of the region where the z-component of the magnetization (m_z) is equal to zero. These values were obtained measuring the width at half-maximum (FWHM) of the profile of m_z along the diameter of the disk, and their values are shown in Fig. 5. The values of the diameters decrease with the increase of the K_z. For example, for $D_{int} = 3\,mJ/m^3$, we have obtained a decrease of approximately 80%, from $D_N \approx 36\,nm$ ($K_z = 0.4\,MJ/m^3$) to $D_N \approx 8\,nm$ ($K_z = 1\,MJ/m^3$). The same behavior occurs for the different values of D_{int}. However, the values of D_N increase with the values of D_{int} for the same values of K_z. For example, for $K_z = 1\,MJ/m^3$, D_N increases from $D_N \approx 7.7\,nm$ ($D_{int} = 3\,mJ/m^3$) to $D_N \approx 34.7\,nm$ ($D_{int} = 3\,mJ/m^3$). These behaviors are expected due to the fact that the increase of K_z favors the perpendicular alignment of the magnetic moments, thus decreasing the region where $m_z = 0$, whereas the increase of D_{int} favors the tilting of magnetic moments, increasing the region where $m_z = 0$.

The minimum values of D_N, for all combinations of D_{int} and K_z, occur in a range between approximately 5 nm and 7 nm (see Fig. 5), whereas the maximum value obtained of D_N was of approximately 36 nm, corresponding approximately to 40% of the diameter of the nanodisk.

In the cases where two skyrmions were obtained in the nanodisk, both have the same D_N, whose value is the same as in the case of a single skyrmion, approximately $D_N \approx 13\,nm$.

Although the Néel skyrmions are metastable, we can see that the values of D_N follow the same behavior as in the cases where the skyrmion is a ground state magnetic configuration [30].

We have found that the values of D_N do not depend on either current densities (J_1 and J_2), or duration times of pulse currents. They dependent only on K_z and D_{int}. This case contrasts with the case where the polarized pulse current density has polarization in the direction $\mathbf{m}_p = (0,0,1)$ [7,18].

3. Coupled nanodisks

In order to study the effect of the dipolar magnetic interaction on the creation of skyrmions, we considered a pair of coupled nanodisks (see Fig. 6). We used the same values of K_z and D_{int} shown in Fig. 2. The currents J_1 and J_2 were applied simultaneously in both nanodisks, in the same way as in the case of an isolated nanodisk (previous section). We

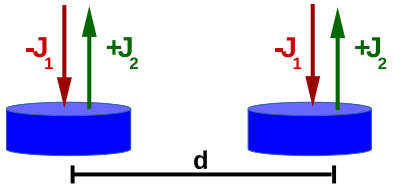

Fig. 6. Schematic representation of a pair of nanodisks separated by a center to center distance d.

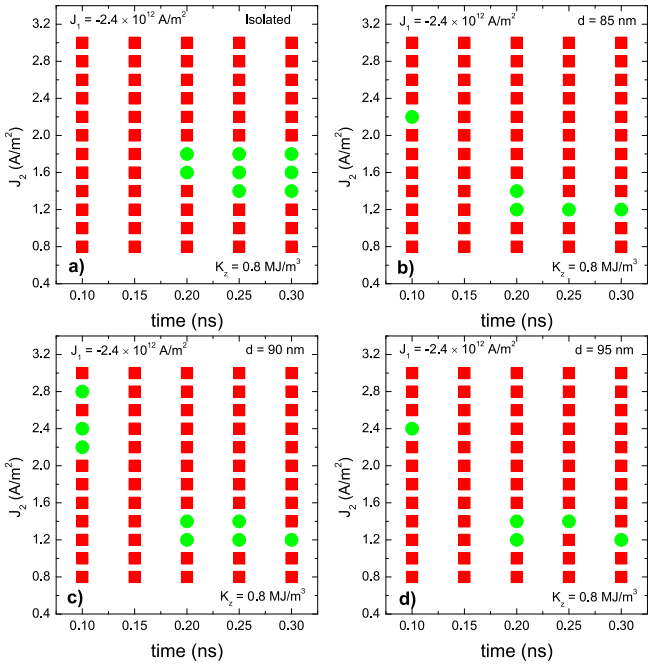

Fig. 7. Phase diagram of J_2 versus its duration, for $K_z = 0.8\,MJ/m^3$ and $D_{int} = 3\,mJ/m^2$, for a) one isolated nanodisk; b) two nanodisks, separation d = 85 nm; c) two nanodisks, d = 90 nm; d) two nanodisks, d = 95 nm. Red squares indicate no creation of skyrmions in either of the two nanodisks, and green circles indicate creation of skyrmions in both nanodisks. (For interpretation of the references to colour in this figure legend, the reader is referred to the web version of this article.)

have considered center to center distances d = 85 nm, 90 nm and 95 nm.

In this case, the phase diagrams for $D_{int} = 3\,mJ/m^2$, $K_z = 0.8\,MJ/m^3$ and $J_1 = -2.4 \times 10^{12}\,A/m^2$ are shown in Fig. 7. It is possible to observe how the phase diagrams change for different values of the distance d. In some cases, the magnetic interaction favors the creation of skyrmions, and in other cases it does not. For example, using a value of $J_2 = 2.2 \times 10^{12}\,A/m^2$, and for any value of duration time of J_2, it is impossible to create a skyrmion (Fig. 7(a)) in an isolated nanodisk, but in a coupled system, it is possible to create a skyrmion for separation distances of d = 85 nm (Fig. 7(b)) and d = 90 nm (Fig. 7(c)), using a duration time of J_2 of t = 10 ns.

The opposite behavior occurs when $J_2 = 1.8 \times 10^{12}\,A/m^2$. In this case, it is possible to create the skyrmion in an isolated nanodisk (Fig. 7(a)) for duration time of J_2 from t = 0.20 ns, 0.25 ns and 0.30 ns, but it is impossible to create the skyrmion when the nanodisks are coupled (Fig. 7(b)–(d)) for any value of duration time of J_2.

The average Néel skyrmion diameters (D_N) neither depend on the magnetic interaction nor on the values of J_1 and J_2. They have almost the same values as in the case of an isolated nanodisk, and have the same dependence on K_z and D_{int}, as shown in Fig. 5. The phase diagrams for the coupled systems are also dependent on the values of J_1. In Fig. 8, we show the phase diagrams for a value of $J_1 = -1.8 \times 10^{12}\,A/m^2$. The phase diagrams are different from those obtained for the case

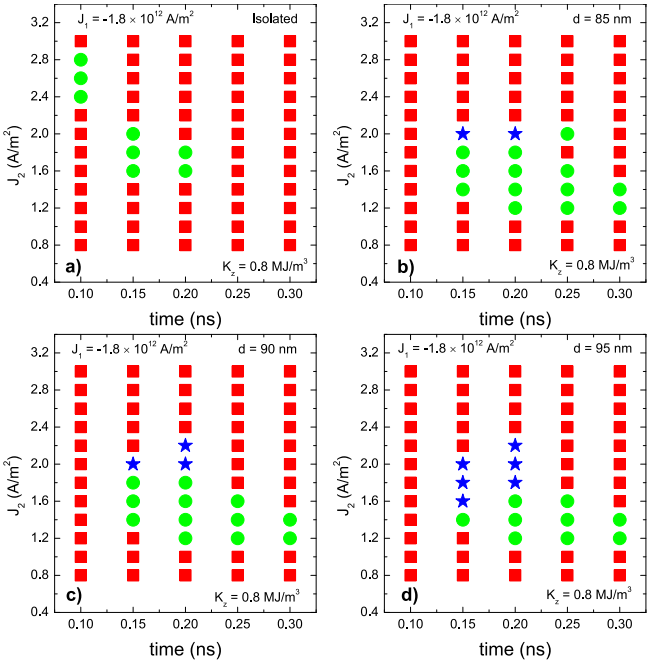

Fig. 8. Phase diagram for $K_z = 0.8\,MJ/m^3$ and $D_{int} = 3\,mJ/m^2$ for (a) one isolated nanodisk; (b) two nanodisks, separation d = 85 nm; (c) two nanodisks, d = 90 nm; (d) two nanodisks, d = 95 nm. Red squares indicate no creation of skyrmion in either of the two nanodisks, blue stars indicate the creation of skyrmion in one of the two nanodisks, and green circles indicate creation of skyrmions in both nanodisks. (For interpretation of the references to colour in this figure legend, the reader is referred to the web version of this article.)

$J_2 = -2.4 \times 10^{12}\,A/m^2$ (Fig. 7).

These diagrams are more complex than the phase diagrams shown in Fig. 7. Besides the cases where skyrmions are present or absent in both nanodisks, there are cases where it was possible to create a skyrmion only in one of the nanodisks. The behavior of the current density threshold of $|J_1|$ (see Fig. 12 in SP) is the same as in the case of an isolated nanodisk. We can see that the threshold of $|J_1|$ decreases with the increase of D_{int} and $|J_1|$ increases with the increase of K_z. The quantitative values of $|J_1|$ are almost the same as those in the case of an isolated nanodisk.

The results shown in Figs. 7 and 8 prove that the magnetic interaction plays an important role in the process of creation of skyrmions in nanodisks. In order to further explore the effects of the dipolar magnetic interaction, we have additionally also considered one triangular array[8] of nanodisks, as shown in Fig. 9.

The phase diagram of current density J_2 versus its duration, for $K_z = 0.8\,MJ/m^3$, $D_{int} = 3\,mJ/m^2$, $J_1 = -2.4 \times 10^{12}\,A/m^2$, are shown in Fig. 10. In this figure, it is possible to observe that the creation of skyrmions in the nanodisks is different for different distances d.

The nanodisks in the triangular array interact in a different form from the case of a pair of coupled nanodisks. For example, for a pair of coupled nanodisks, with parameters: $J_2 = 2.2 \times 10^{12}\,A/m^2$, t = 0.10 ns and distance d = 85 nm, the skyrmions can be created in both nanodisks (Fig. 7(b)), while for the same parameters, for a triangular array, the skyrmions cannot be created in the three nanodisks (Fig. 10(a)). Also, a similar behavior can be seen for $J_2 = 2 \times 10^{12}\,A/m^2$ and distance d = 85 nm (Fig. 7(b)), while for a pair of coupled nanodisks, the magnetic interaction prevents the creation of skyrmions in the whole range of values of duration of J_2, this magnetic interaction favors the creation of skyrmions in two of three nanodisks (Fig. 10(a)).

[8] The procedure to obtain the skyrmion is the same as in the previous cases.

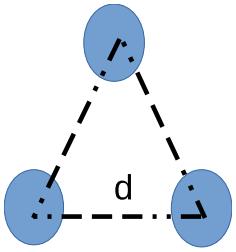

Fig. 9. Schematic representation of an equilateral triangular array of coupled nanodisks separated by a center to center distance d.

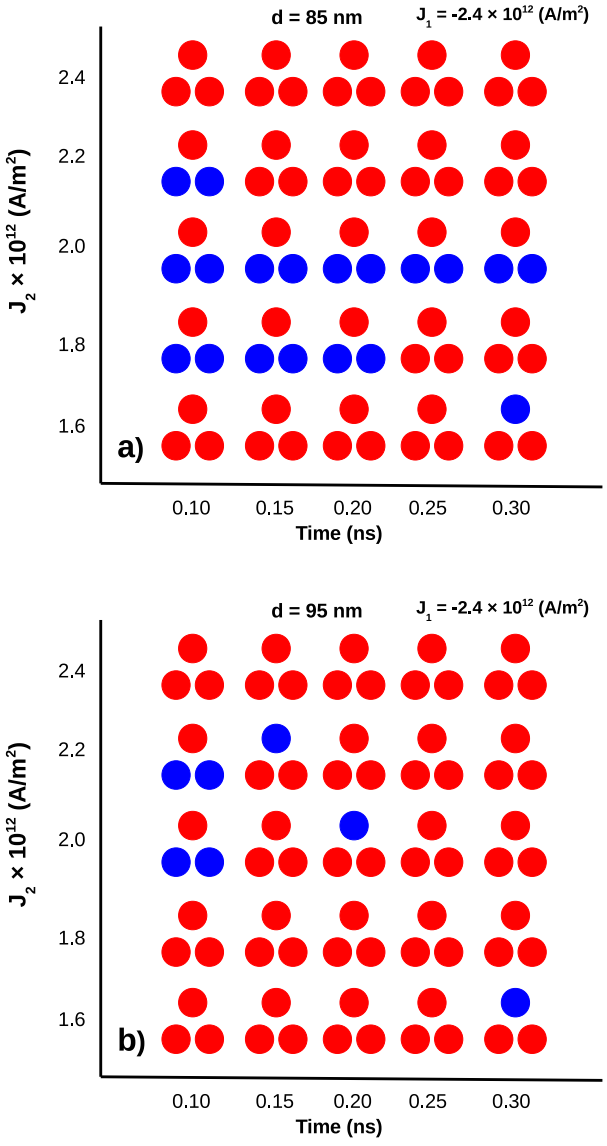

Fig. 10. Phase diagram, of current density J_2 versus its duration, for a triangular array, for $K_z = 0.8\,MJ/m^3$ and $D_{int} = 3\,mJ/m^2$. Red circles indicate the nanodisk where there is no creation of skyrmions, blue circles indicate the nanodisk where there is creation of skyrmions. (For interpretation of the references to colour in this figure legend, the reader is referred to the web version of this article.)

4. Conclusions

In this work, we have studied the influence of the magnetic interaction in the creation of a metastable skyrmion in isolated and coupled systems of nanodisks, through pulsed spin current densities, using micromagnetic simulation. We have built phase diagrams to show under what conditions it is possible to obtain a skyrmion. Although our phase diagrams do not show a direct relationship between the parameters used here, we have been able to find some general behavior such as the fact that the threshold J_1 increases with the increase of the anisotropy, and decreases with the increase of D_{int}. Our results show that the diameters of the metastable skyrmions have the same behavior as D_N of stable skyrmions.

We have demonstrated that, in the case of coupled systems, the magnetic interaction plays an important role in the creation of metastable skyrmions, modifying the phase diagrams when the distance between the nanodisks is changed. However, the magnetic interaction does not modify the values of the threshold of the current density J_1.

Our results show an effect not sufficiently studied, the influence of the dipolar magnetic interactions in the creation of skyrmions, and opens the door for future studies on how the magnetic interaction between the disks changes over time during the process of creation of a skyrmion.

Acknowledgments

The authors would like to thank the support of the Brazilian agencies FAPERJ and CNPq.

Appendix A. Supplementary data

Supplementary data associated with this article can be found, in the online version, at https://doi.org/10.1016/j.jmmm.2019.165406.

References

[1] S. Seki, M. Mochizuki, Skyrmions in Magnetic Materials, first ed., Springer, Cham, 2016.
[2] A.P. Guimarães, Principles of Nanomagnetism, second ed., Springer, Cham, 2017.
[3] J. Sampaio, V. Cros, S. Rohart, A. Thiaville, A. Fert, Nucleation, stability and current-induced motion of isolated magnetic skyrmions in nanostructures, Nat. Nanotechnol. 8 (2013) 839–844, https://doi.org/10.1038/nnano.2013.210.
[4] G. Finocchio, F. Büttner, R. Tomasello, M. Carpentieri, M. Kläui, Magnetic skyrmions: from fundamental to applications, J. Phys. D: Appl. Phys. 49 (42) (2016) 423001,, , https://doi.org/10.1088/0022-3727/49/42/423001.
[5] S. Chen, Q. Zhu, S. Zhang, C. Jin, C. Song, J. Wang, Q. Liu, Dynamic response for Dzyaloshinskii-Moriya interaction on bubble-like magnetic solitons driven by spin-polarized current, J. Phys. D: Appl. Phys. 49 (19) (2016) 195004, , https://doi.org/10.1088/0022-3727/49/19/195004.
[6] Y. Yamane, J. Sinova, Skyrmion-number dependence of spin-transfer torque on magnetic bubbles, J. Appl. Phys. 120 (23) (2016) 233901, , https://doi.org/10.1063/1.4971868.
[7] R.L. Novak, F. Garcia, E.R.P. Novais, J.P. Sinnecker, A.P. Guimarães, Micromagnetic study of skyrmion stability in confined magnetic structures with perpendicular anisotropy, J. Magn. Magn. Mater. 451 (2018) 749–760, https://doi.org/10.1016/j.jmmm.2017.12.004.
[8] K.Y. Guslienko, Néel skyrmion stability in ultrathin circular magnetic nanodots, Appl. Phys. Express 11 (6) (2018) 063007.
[9] J. Kim, J. Yang, Y.-J. Cho, B. Kim, S.-K. Kim, Coupled breathing modes in one-dimensional skyrmion lattices, J. Appl. Phys. 123 (2018) 053903, , https://doi.org/10.1063/1.5010948.
[10] X. Zhang, M. Ezawa, Y. Zhou, Magnetic skyrmion logic gates: conversion, duplication and merging of skyrmions, Scientific Rep. 5 (2015) 9400, https://doi.org/10.1038/srep09400.
[11] R. Tomasello, E. Martinez, R. Zivieri, L. Torres, M. Carpentieri, G. Finocchio, A strategy for the design of skyrmion racetrack memories, Scientific Rep. 4 (2014) 6784, https://doi.org/10.1038/srep06784.
[12] S. Zhang, J. Wang, Q. Zheng, Q. Zhu, X. Liu, S. Chen, C. Jin, Q. Liu, C. Jia, D. Xue, Current-induced magnetic skyrmions oscillator, New J. Phys. 17 (2) (2015) 02306110.1088/1367-2630/17/2/023061.
[13] Y. Liu, H. Yan, M. Jia, H. Du, A. Du, J. Zang, Field-driven oscillation and rotation of a multiskyrmion cluster in a nanodisk, Phys. Rev. B 95 (2017) 134442, , https://doi.org/10.1103/PhysRevB.95.134442.
[14] N. Del-Valle, S. Agramunt-Puig, A. Sanchez, C. Navau, Imprinting skyrmions in thin films by ferromagnetic and superconducting templates, Appl. Phys. Lett. 107 (13) (2015) 133103, , https://doi.org/10.1063/1.4932090.
[15] V. Flovik, A. Qaiumzadeh, A.K. Nandy, C. Heo, T. Rasing, Generation of single skyrmions by picosecond magnetic field pulses, Phys. Rev. B 96 (2017) 140411, , https://doi.org/10.1103/PhysRevB.96.140411.
[16] M. Mochizuki, Controlled creation of nanometric skyrmions using external magnetic fields, Appl. Phys. Lett. 111 (9) (2017) 092403, , https://doi.org/10.1063/1.

4993855.
[17] S.-Z. Lin, C. Reichhardt, A. Saxena, Manipulation of skyrmions in nanodisks with a current pulse and skyrmion rectifier, Appl. Phys. Lett. 102 (22) (2013) 222405, , https://doi.org/10.1063/1.4809751.
[18] H.Y. Yuan, X.R. Wang, Skyrmion creation and manipulation by nano-second current pulses, Scientific Rep. 6 (2016) 22638, , https://doi.org/10.1038/srep22638.
[19] W. Koshibae, N. Nagaosa, Creation of skyrmions and antiskyrmions by local heating, Nat. Commun. 5 (2014) 5148, , https://doi.org/10.1038/ncomms6148.
[20] X. Zhang, Y. Zhou, M. Ezawa, High-topological-number magnetic skyrmions and topologically protected dissipative structure, Phys. Rev. B 93 (2016) 024415, , https://doi.org/10.1103/PhysRevB.93.024415.
[21] F. Jonietz, S. Mühlbauer, C. Pfleiderer, A. Neubauer, W. Münzer, A. Bauer, T. Adams, R. Georgii, P. Böni, R.A. Duine, K. Everschor, M. Garst, A. Rosch, Spin transfer torques in MnSi at ultralow current densities, Science 330 (6011) (2010) 1648–1651, https://doi.org/10.1126/science.1195709.
[22] J. Müller, Magnetic skyrmions on a two-lane racetrack, New J. Phys. 19 (2) (2017) 025002, , https://doi.org/10.1088/1367-2630/aa5b55.
[23] F. Garcia-Sanchez, J. Sampaio, N. Reyren, V. Cros, J.-V. Kim, A skyrmion-based spin-torque nano-oscillator, New J. Phys. 18 (7) (2016) 075011, , https://doi.org/10.1088/1367-2630/18/7/075011.
[24] S. Zhang, J. Wang, Q. Zheng, Q. Zhu, X. Liu, S. Chen, C. Jin, Q. Liu, C. Jia, D. Xue, Current-induced magnetic skyrmions oscillator, New J. Phys. 17 (2) (2015) 0230611367-2630/17/2/023061.
[25] C.P. Chui, Y. Zhou, Skyrmion stability in nanocontact spin-transfer oscillators, AIP Adv. 5 (9) (2015) 097126, , https://doi.org/10.1063/1.4930904.
[26] S.I. Kiselev, J.C. Sankey, I.N. Krivorotov, N.C. Emley, R.J. Schoelkopf, R.A. Buhrman, D.C. Ralph, Microwave oscillations of a nanomagnet driven by a spin-polarized current, Nature 425 (2003) 380, https://doi.org/10.1038/nature01967.
[27] N. Vidal-Silva, A. Riveros, J. Escrig, Stability of Néel skyrmions in ultra-thin nanodots considering Dzyaloshinskii-Moriya and dipolar interactions, J. Magn. Magn. Mater. 443 (2017) 116–123, https://doi.org/10.1016/j.jmmm.2017.07.049.
[28] A. Vansteenkiste, J. Leliaert, M. Dvornik, M. Helsen, F. Garcia-Sanchez, B. Van Waeyenberge, The design and verification of Mumax3, AIP Adv. 4 (2014) 107133, , https://doi.org/10.1063/1.4899186.
[29] A. Talapatra, J. Mohanty, Scalable magnetic skyrmions in nanostructures, Comput. Mater. Sci. 154 (2018) 481–487, https://doi.org/10.1016/j.commatsci.2018.08.022.
[30] S. Rohart, A. Thiaville, Skyrmion confinement in ultrathin film nanostructures in the presence of Dzyaloshinskii-Moriya interaction, Phys. Rev. B 88 (2013) 184422, , https://doi.org/10.1103/PhysRevB.88.184422.